

# Disentangling the albedo of the exoplanets from the stellar activity.

Luisa Maria Serrano<sup>1,2</sup>,

<sup>1</sup> Instituto de Astrofísica e Ciências do Espaço, Universidade do Porto, CAUP, Rua das Estrelas, PT4150-762 Porto, Portugal

<sup>2</sup> Departamento de Física e Astronomia, Faculdade de Ciências, Universidade do Porto, Rua de Campo Alegre, 4169-007 Porto, Portugal

## Abstract

The stellar phase curves of stars orbited by one planet include, in realistic conditions, the primary and secondary transit, three secondary effects, which are the beaming effect, the ellipsoidal modulation and the reflected light component of the planet, plus two sources of noise, the stellar activity and the instrumental noise. In our paper 'Distinguishing the albedo of the exoplanets from the stellar activity' we aimed at analyzing whether it was possible to detect the reflected light component of a planet in the case of an active bright star and supposing the instrumental noise to be on the same level of the predicted one for CHEOPS mission. The results of our work are important for planning observations of phase curves with CHEOPS and also with other future photometric missions.

## 1 Introduction

The study of planetary atmospheres is an up-rising field of planetary characterization and it includes different techniques. One of them consists of analyzing the photometric emission of a star to retrieve the planetary albedo [3, 1].

A phase light curve is the flux emitted by the planetary system as a function of time. For a quiet star, it includes the primary transit, which happens when the planet crosses the stellar disc, the secondary eclipse, when the planet passes behind the star, and three weaker modulations. The first one is the doppler beaming effect, which consists of a change in the stellar brightness, proportional to the radial velocity amplitude of the planet. The second phenomenon is the ellipsoidal modulation, a shape modification of the star, which is deformed due to the gravitational attraction of the orbiting planet. The last component is the planetary flux, which includes the thermal proper emission of the planetary atmosphere

and the reflected light component (the stellar light reflected by the planetary atmosphere). The thermal flux is stronger in the infrared observations, while the reflection dominates in the optical.

The future mission CHEOPS [5], which will be launched at the end of this year, among its secondary objectives, has the aim of analyzing the phase curves of exoplanets. Since CHEOPS observations will be performed in the optical domain, they will slightly be affected by the planetary thermal emission. The planetary flux will be dominated by the reflected component, which is proportional to the atmospheric albedo. Measuring the albedo is possible, but hampered by the two main sources of noise, the instrumental noise and the stellar activity, in the form of spots and plages [7]. Past works were capable to measure the albedo of hot Jupiters and some Neptunes, especially if observed with Kepler, because they had at disposition long observational periods [1, 3, 6]. Thus, by phase-folding the light curves, the instrumental error decreases and the albedo can be estimated with a high precision. CHEOPS will have a lower instrumental noise than Kepler, but, being an in-space telescope, it will have a limited time of observation for each target, maximum 20 days. Thus, applying the phase folding technique for determining the albedo of the planets observed with CHEOPS will not be possible. Serrano et al. 2018 [11] analyzed synthetic light curves adopting an MCMC which describes the stellar activity with a Gaussian Process. They demonstrated that with CHEOPS predicted level of noise and considering a maximum period of observation of 20 days (as programmed for each target observed with CHEOPS), it is possible to measure the albedo, distinguishing the reflected light component of the planet from the stellar activity, if the star is bright and the observations cover at least one entire stellar period of rotation.

## 2 Synthetic light curves and fitting method

Serrano et al. 2018 [11] produced simulations of phase light curves which included three main components: the reflected light component of the planet, the instrumental error and the stellar activity. They did not include the primary transit to focus the entire analysis on the reflected light component and how much the stellar activity can absorb it, hampering its detection. The secondary eclipse was also not included in the model because it is not always identified due to the stellar activity (see [6]). Moreover, not accounting for the two eclipses, they also tested the opportunity to detect non-transiting planets through their reflected light component, as suggested by Crossfield et al. 2010 [2]. For example, some planets, discovered through the radial velocity technique, do not transit their parent star because of the high orbital inclination. For this specific cases, the only way to study the atmosphere is through the reflected light component.

For modelling the reflected light component they adopted the lambertian model, which describes the planet as an isotropically reflecting sphere. The expression is:

$$\frac{F_p}{F_*} = A_g \left( \frac{R_p}{a} \right)^2 \frac{\sin z - (\pi - z) \cos z}{\pi} \quad (1)$$

with  $F_p$  the planetary flux,  $F_*$  the stellar flux,  $A_g$  the geometric albedo,  $R_p$  the radius of the planet,  $a$  the semi-major axis and  $z$  depends on the orbital inclination  $i$  and on the orbital

phase.

For the stellar activity, the tool SOAP-T [8] was adopted to produce an activity pattern with an amplitude similar to those of moderately active stars. The instrumental noise was modelled as a white noise, with standard deviation equal to the predicted level of noise for CHEOPS. The produced simulations are characterized by 2 hours of timing. The reason of this choice is that, even if CHEOPS will have a timing of one point per minute, for data with shorter time periods than 2 hours, other stellar surface phenomena become significant (granulation for instance). Binning should help to reduce these extra noise sources. This said, CHEOPS predicted level of noise in 2 hours is 14 *ppm* for a 6.5 magnitude star, 17 *ppm* for an 8 magnitude star and 29 *ppm* if the magnitude is 10.

The final simulations are obtained by summing the three components:

$$\frac{F_{total}}{F_*} = \frac{F_p}{F_*} + \frac{F_{*,spotted}}{F_*} + \frac{F_{noise}}{F_*} \quad (2)$$

with  $F_{*,spotted}$  the activity pattern and  $F_{noise}$  the instrumental noise.

Serrano et al. 2018 [11] adopted a Markov Chain Montecarlo (MCMC) as a fitting analysis method to recover the albedo, distinguishing it from the stellar activity. Modeling the stellar activity with an analytical model is not recommendable, given the high degeneracy of the problem. For this reason, the best approach so far developed consists of applying a Gaussian Process (GP), which treats the stellar activity as a correlated noise. As covariance function, the usual choice was the quasi periodic [4]. Since *SOAP-T* does not account for spot evolution, the chosen covariance function was totally periodic. Thus, the MCMC used the GP with periodic kernel to model the stellar activity and it adopted as fitting model the reflected light component of the exoplanet.

To sample from the posterior distributions the authors ran the tool *emcee*, which performs the MCMC. The estimated parameters were 5: the geometric albedo  $A_g$ , the stellar rotation  $P_*$ , the amplitude of the correlation  $p_1$ , the timescale decay of the periodic modulation  $p_2$ , and an offset to fit the average value of the light curve. All the other planetary and stellar parameters were supposed to be known (for example with a transit or other detection methods), and thus fixed in the tests. For the albedo  $A_g$  and the offset the authors chose uniform priors, for the hyperparameters of the periodic kernel log-uniform priors, while for  $P_*$  a gaussian prior, centered on a previously estimated value. The stellar rotation is not always known, but some estimations can always be performed maybe with lomb-scargle periodogram or even an MCMC without imputing the reflected light component.

Each run of the MCMC required 30 chains from the prior distribution. A 500-step burn-in was performed, followed by a 1000 steps chains sampling. Thus, for each simulation the authors could obtain 30000 effective samples from the posterior distribution functions. The medians of the posterior distributions represented the best fit values of the free parameters. The  $1\sigma$  uncertainties were the differences between the best-fit value and the 16<sup>th</sup> and 84<sup>th</sup> percentiles, respectively.

Table 1: Stellar and planetary properties adopted as starting parameters for the tests.

Stellar radius	$R_*$	$1 R_\odot$
Stellar inclination	$I$	$90^\circ$
Stellar temperature	$T_*$	5778 K
Linear limb-darkening coefficient	$c_1$	0.29
Quadratic limb-darkening coefficient	$c_2$	0.34
Planet radius	$R_p$	$0.1 R_*$
Time of mid-transit	$t_0$	0.2 days
Eccentricity	$e$	0
Argument of periastron	$w$	$0^\circ$
Inclination of the orbital plane	$i$	$90^\circ$
Projected spin-orbit misalignment angle	$\lambda$	$0^\circ$
Albedo	$A_g$	0.3

### 3 Minimum observation length for a target

Serrano et al. 2018 [11] produced simulations of stars with one orbiting planets, with the properties listed in table 1 for the planetary characteristics. For the spots properties refer to table 6 in [11]. The simulations had increasing durations, starting with one covering an entire orbital period and then augmenting by 3 days each time. The maximum observation length was 60 *days*. They performed this test for five different stellar rotational periods, 7, 11, 19, 23 and 26 *days*. The results are reported in the left side of figure 1, which shows the albedo as a function of the number of stellar rotations. For observation lengths shorter than the rotational period of the star, the *MCMC* cannot recover the albedo. After 1 stellar rotation, the errorbars significantly decrease and the albedo becomes closer to the inputed one. For more than 2  $P_*$  the values are compatible to the real ones within  $1\sigma$ . The main reason for this is that the albedo cannot be estimated without knowing well the stellar period of rotation,  $P_*$ . The Gaussian Process uses a periodic kernel for the activity and thus it needs observations longer than  $P_*$  itself, to predict it. There is also a duality between fast and slow rotators, with the 7- and 11 - *days* cases which converge to the inputed values well after 2 rotational periods. The other cases, instead, show a faster convergence, probably because for longer period of rotation, the rotation covers a longer time span and is described by more data points.

We can conclude that accounting for 20 *days* maximum period of observation with CHEOPS it is possible to measure the albedo for stars with a maximum period of rotation of 19 *days*. For fast rotators it would be better to cover all the 20 *days* of observations, or also decreasing the binning could be a solution. Serrano et al. 2018 [11] showed that for the 11 - *days* case, binning to 30 minutes the data instead of 2 hours, helps to get better albedo parameter after one stellar rotation, because the number of data points increases. It is important, anyway, to be careful with this smaller binning, because other activity features might rise, like the granulation.

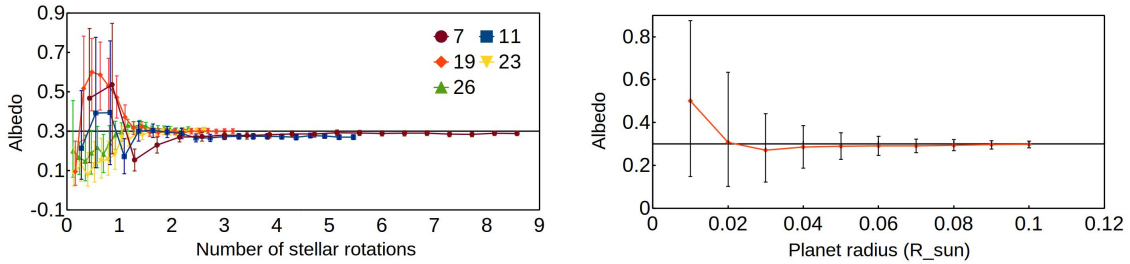


Figure 1: In the left, plot of the albedo and relative errors for the simulations obtained with  $P_* = 7, 11, 19, 23,$  and  $26$  days and increasing observational lengths. In the right, plot of the recovered albedo as a function of the planetary radius. These plots are taken from Serrano et al. 2018 [11].

## 4 Other results

Serrano et al. 2018 [11] also tested how the precision of the albedo estimation changes by varying other parameters. To do this, they fixed the length of the simulations to  $39$  days and the stellar period of rotation to  $19$  days.

Increasing the stellar magnitude, thus the amplitude of the instrumental noise, the convergence to the inputted albedo happens later than the 2 rotations boundary. For example, with  $29$  ppm of noise the stabilization is reached after  $2.5$  days.

Then, they varied the orbital period, increasing it of  $1$  day from  $3$  days until  $15$  days. As the period of the planet increases, the error of the identified albedo also increases. Increasing the period, indeed, lowers the signal of the planet and a longer time of observation is necessary to measure it.

Serrano et al. 2018 [11] also varied the planet radius from  $0.1 R_*$  to  $0.01 R_*$  and found that the albedo can still be measured until the regime of small neptunes, with  $R_p = 0.04 R_*$  (see the right side of figure 1). They additionally fixed  $R_p$  to  $0.1 R_*$  and  $0.05 R_*$  and varied the albedo from  $0.6$  to  $0$ . Fitting them with the MCMC, they got the correct albedo and did not observe strong error variations between the different values, both for Jupiter size planets and Neptun size planets.

Finally, they varied the activity pattern by multiplying it by  $100, 10, 5$  and  $0.1$  and adding  $-99, -9, -4,$  and  $0.9$  respectively. Applying their MCMC, they demonstrated that once the activity pattern is well described by the kernel of the GP, the albedo is always retrieved. Thus, with this technique even if the star is very active, determining the planetary albedo is always possible. The main issue remains the instrumental noise.

## 5 Applying to real data

Serrano et al. 2018 [11] performed two different types of tests on real data. In the first one, they chose a periodic star from the McQuillan database of periodic stars, KIC 3643000,

and they selected a portion of the light curve of the star in which the stellar activity does not significantly change. They added a planetary phase curve to this star, with the same properties as in table 1. They binned the data to have the same sampling as before and they obtained as level of noise 39 *ppm*, higher than the predicted one for CHEOPS. They applied the fitting tool on the phase curve and they got  $A_g = 0.26 \pm 0.11$ . The errorbar is twice the one obtained in the simulations. Apart from the instrumental noise, the main reason is connected to the kernel of the GP, which is periodic, while the stellar activity in the analyzed data is not exactly periodic. So, an aperiodic kernel would have probably helped to get a more precise result.

This is confirmed by the test performed on the star Kepler-7, which has a hot Jupiter orbiting around, Kepler-7b. This target was first analyzed by Angerhausen et al. 2015 [1], who retrieved an albedo of 0.35. Serrano et al. 2018 [11] extracted the entire 10th quarter of Kepler observations and binned the data to two hours. They applied their fitting tool and retrieved  $A_g = 0.36$ , close to the value found by Angerhausen et al. 2015 [1]. Anyway, the rotation period of the star results to be lower than the measured one (15.7 *days* instead of 16.7) and the hyper-parameters  $p_1$  and  $p_2$  are also physically poorly constrained. The fitted activity is not as periodic as it should be, given the adopted kernel, because Kepler-7 activity is not strictly periodic and shows evidence of spot evolution.

We can conclude that the fitting tool right now does not work for real data, because it requires the aperiodic component in the kernel of the GP. Nonetheless, once improved the tool with CHEOPS we will have the opportunity to measure the albedo of several Jupiter size planets and some small Neptunes. Much better results are instead expected with the launch of future photometric missions, like TESS [10] and PLATO [9], because their instrumental noise is lower and they will offer long periods of observations, thus allowing for data covering many stellar rotations. Using the GP for modelling the activity will allow to get rid of the extra noise which did not permit so far to measure the albedo of planets orbiting active stars.

## Acknowledgments

This work was supported by Fundação para a Ciência e Tecnologia (FCT) through national funds and by FEDER through COMPETE2020-Programa Operacional Competitividade e Internacionalização by these grants UID/FIS/04434/2013 & POCI-01-0145-FEDER-007672; PTDC/FIS-AST/28953/2017 & POCI-01-0145-FEDER-028953 and PTDC/FIS-AST/32113/2017 & POCI-01-0145-FEDER-032113.

L.M.S. also acknowledges support by the fellowship SFRH/BD/120518/2016 funded by FCT (Portugal) and POPH/FSE (EC).

## References

- [1] Angerhausen, D., DeLarme, E., & Morse, J. A. 2015, *PASP*, 127, 1113
- [2] Crossfield, I. J. M., Hansen, B. M. S., Harrington, J., et al. 2010, *ApJ*, 723, 1436

- [3] Esteves, L. J., De Mooij, E. J. W., & Jayawardhana, R. 2013, *ApJ*, 772, 51
- [4] Faria, J. P., Haywood, R. D., Brewer, B. J., et al. 2016, *A&A*, 588, A31
- [5] Fortier, A., Beck, T., Benz, W., et al. 2014, in *Proc. SPIE*, Vol. 9143, *Space Telescopes and Instrumentation 2014: Optical, Infrared, and Millimeter Wave*, 91432J
- [6] Lillo-Box, J., Barrado, D., Moya, A., et al. 2014, *A&A*, 562, A109
- [7] Oshagh, M., Santos, N. C., Ehrenreich, D., et al. 2014, *A&A*, 568, A99
- [8] Oshagh, M., Boisse, I., Boué, G., et al. 2013a, *A&A*, 549, A35
- [9] Rauer, H., Aerts, C., Cabrera, J., & PLATO Team. 2016, *Astronomische Nachrichten*, 337, 961
- [10] Ricker, G. R., Winn, J. N., Vanderspek, R., et al. 2015, *Journal of Astronomical Telescopes, Instruments, and Systems*, 1, 014003
- [11] Serrano, L. M., Barros, S. C. C., Oshagh, M., et al. 2018, *A&A*, 611, A8